IEEE Access
Multidisciplinary | Rapid Review | Open Access Journal

Received November 27, 2020, accepted December 2, 2020, date of publication December 8, 2020,
date of current version December 30, 2020.

Digital Object Identifier 10.1109/ACCESS.2020.3043370

Cooperative Adaptive Cruise Control Strategy Optimization for Electric Vehicles Based on SA-PSO With Model Predictive Control

HAO MA, LIANG CHU, (Member, IEEE), JIANHUA GUO, JIAWEI WANG, AND CHONG GUO
State Key Laboratory of Automotive Dynamic Simulation and Control, Jilin University, Changchun 130022, China

Corresponding author: Jianhua Guo (xhhmail@jlu.edu.cn)

This work was supported in part by the Jilin Science and Technology Development Plan Project under Grant 20170204085GX, in part by the 863 National High Technology Research and Development Program of China under Grant 2012AA110903, in part by the National Natural Science Foundation of China under Grant 51405075 and Grant 51775238, and in part by the Jilin Industrial Technology Innovation Strategic Alliance Project under Grant 20150309013GX.

ABSTRACT The Cooperative Adaptive Cruise Control (CACC) is considered to be an effective method to improve traffic flow. However, the comfortability and economy need to be paid more attention to besides stability and safety. In this paper, a CACC strategy is proposed for an electric vehicle platoon to improve the economy, following performance, safety, and comfortability characteristics, based on the model predictive control (MPC) with simulated annealing-particle swarm optimization (SA-PSO) algorithm. Firstly, the braking force distribution strategy of electric vehicles is designed to improve the efficiency of regenerative braking. Secondly, based on the variable vehicle spacing with fixed time headway, a vehicle platoon following strategy is established to meet the following performance and safety. Thirdly, an MPC controller is used to control the states of the vehicles in the platoon to satisfy the performance. A multi-objective function of the MPC controller is established, including the economy, following performance, comfortability, and safety of the vehicles in the platoon. The SA-PSO algorithm effectively solves the problem of the discrete variables in the objective function. Simulations are conducted to validate the sufficient conditions of the economy, following performance, comfortability, and safety. Simulation results demonstrate that the economic efficiency of the CACC strategy with the economic index is 16.5% higher than that of the existing ACC strategy. Meanwhile, the other characteristics can also meet the control requirement.

INDEX TERMS Cooperative adaptive cruise control, simulated annealing, particle swarm optimization, vehicle platoon, electric vehicle, model predictive control.

I. INTRODUCTION

With the development of the automotive industry and the growth of social car ownership, the contradiction between the increasing number of road vehicles and the restriction of urban traffic and highway load is also intensifying. Drivers need to know more about their driving environment to plan the driving route better and improve driving safety and comfortability. In this context, it is necessary to introduce advanced driver assistance systems (ADAS) into automotive technology. There are two primary development directions of ADAS: one is to realize the interconnection from vehicle to vehicle (V2V), vehicle to infrastructure(V2I), and from infrastructure to vehicle (I2V); the other is to realize the adaptive cruise control (ACC). Cooperative adaptive cruise control (CACC) can be regarded as a combination of the V2V and ACC [1], [2].

The cooperative adaptive cruise control (CACC) problem is the extension of the adaptive cruise control (ACC) problem. The ACC strategy adjusts vehicle driving state according to the front situation. When no following target exists, the vehicle will cruise at the speed set by the driver. When the target exists, the controller will correct the speed according to the safety distance to achieve the following-up condition. However, it's easy to cause a time delay as the rear vehicle identifies the state changing of the previous vehicle. When numbers of vehicles turn on ACC mode in the same lane, the time delay of accumulation leads to the oscillation of vehicles. CACC

The associate editor coordinating the review of this manuscript and approving it for publication was Shihong Ding.

can solve the time delay. Based on intelligent vehicle path planning and driving behavior planning, the vehicular networking technology and intelligent transportation technology are introduced to establish real-time information interaction between different vehicles in the platoon to achieve the overall optimal driving strategy of the platoon [3], [4].

The driving control strategy with the ACC system in traffic flow has been extensively studied. Goñi-Ros *et al.* designed an ACC controller for a single vehicle to reduce traffic congestion by adjusting the control parameters such as the desired time interval and space range [5], [6]. Spiliopoulou Anastasia *et al.* used a predictive algorithm controller to estimate fuel consumption at different traffic scenarios in nonlinear and linear systems [6]–[8]. Andreas Weißmann *et al.* designed MPC controllers to get the states of the vehicle in every predictive horizon and adjusted the acceleration and velocity to follow the optimal trajectory [9]–[12]. Wu Yunkai *et al.* designed the MPC algorithm in fault diagnosis and tolerant control [13], [14].

The essence of CACC is that vehicles drive in platoon mode and communicate with each other simultaneously [15]. The advantage of CACC is that it can significantly optimize the driving speed profile and make the driving process more stable [16], [17]. Lidstrom, K, *et al.* developed a longitudinal controller that uses information exchanged via wireless communication with other cooperative vehicles to achieve string-stable platooning [18]. Liu, Yonggui, *et al.* proposed two distributed control protocols in which consider not only lateral control but also longitudinal control [19]. Shet, Rahi Avinash, *et al.* investigated the performance of cruise controls with respect to safety, reliability, passenger comfort and expanded the adaptive cruise control and cooperative adaptive cruise control to a new controller specifically aiming at higher passenger comfort [20]. Li, Ye, et al developed a control strategy of an integrated system of cooperative adaptive cruise control (CACC) and variable speed limit (VSL) to reduce rear-end collision risks near freeway bottlenecks [21]. Zhu Yuanheng *et al.* transformed the non-uniform CACC problem into the error dynamic adjustment problem using the dynamic parameter estimation, and proposed an adaptive optimal control method based on the online data learning optimal feedback [22]. Chang Ben-Jye *et al.* proposed a vehicle group cooperative adaptive driving (CAD) method based on mobile edge computing, which effectively avoided the vibration phenomenon in platoon [23]. The CACC system designed by Milanes Vicente *et al.* is composed of two controllers: one for managing the proximity to the front vehicle and the other for adjusting the vehicle joining the platoon [24].

Van Arem Bart *et al.* designed a traffic flow simulation model called MIXIC to study the impact of the merging scheme from four lanes to three lanes on traffic flow [25]. The results showed that compared with the vehicles without the merging scheme, the stability and efficiency of traffic flow are slightly improved. CACC system achieves good fuel economy. Almannaa *et al.* pointed out that the CACC system can save about 19% of vehicle fuel consumption than drivers in longitudinal control [26]. Zhai, Chunjie, *et al.* proposed an Eco-CACC strategy for a heterogeneous platoon of heavy-duty vehicles with time delays. The Eco-CACC strategy significantly improve the fuel economy of heterogeneous platoon. [27]. Dannheim *et al.* optimized the speed and route of the CACC system [28]. The results showed that the CACC system has a positive impact on the overall carbon dioxide emissions of the platoon.

Most of the above research only solves a specific characteristic of the CACC system (platoon stability, fuel economy, or safety). This paper proposes a multi-objective optimal CACC strategy consisting of the braking force distribution strategy, vehicle platoon following strategy, and MPC controller. Compared with the current work, the main contributions of this paper are as follows:

1) Considering the influence of regenerative braking on the economy, the braking force distribution strategy is formulated in the CACC system;

2) An MPC strategy with multi-objective function including following performance, comfortability, safety, and economy is proposed to improve the drivability of vehicle platoon;

3) The optimal global solution is calculated accurately in the predictive horizon by using the SA-PSO algorithm, and the nonlinear problem of discrete state is solved.

The remainder of this article is organized as follows. Section II presents the longitudinal dynamics model, battery model, and braking force distribution model of the vehicle platoon. Section III presents the vehicle platoon following strategy, and the MPC controller is designed with a multi-objective function and SA-PSO algorithm. Section IV implements a simulation of an electric vehicle platoon based on the proposed CACC strategy and compares the results of ACC and CACC strategy. In section V, the simulation results are discussed, followed by the conclusion of this article.

II. MODELING

This article considers a multi-objective optimization of the platoon. The platoon consists of one lead vehicle and N followers. This section will present the longitudinal dynamics model, battery model, and the braking force distribution model of the vehicle platoon.

A. LONGITUDINAL DYNAMICS MODEL OF VEHICLE PLATOON

This article applies a second-order differential mode to describe the upper-level longitudinal dynamics of vehicles in the platoon. the upper-level longitudinal dynamics model of the vehicle platoon at the time i can be expressed as

$$\begin{cases} \dot{s_h}(i) = v_h(i) \\ \dot{v_h}(i) = a_h(i) \end{cases} \tag{1}$$

where $s_h(i)$, $v_h(i)$ and $a_h(i)$ are the position, velocity, and control input of vehicle h, respectively.

Acceleration can be written as an equation of driving power, braking force, and resistance force. According to

Newton's second law, the relationship among the control input $a_h(i)$, the desired motor output power $P_{h,e}(i)$, the braking force $F_{h,b}(i)$ and the resistance force $F_{h,r}(i)$ can be expressed as

$$a_h(i) = \frac{1}{m_h}\left(\frac{\eta_{h,i}P_{h,e}(i)}{v_h(i)} - F_{h,b}(i) - F_{h,r}(i)\right) \tag{2}$$

where $m_h(i)$ is the mass of vehicle h, and the resistance force $F_{h,r}(i)$ consists of the rolling resistance and wind resistance can be described as

$$F_{h,r}(i) = m_h g f + \frac{C_d \rho A_h v_h^2(i)}{2} \tag{3}$$

where g and f are the gravitational acceleration and rolling coefficient. C_d, ρ and A_h are the drag coefficient, air density, and frontal area.

1) VEHICLE STABILITY

When the speed is stable, the vehicles will maintain the same state as the previous vehicle. The speed is same and the acceleration is zero. All vehicles drive at the expected position, ie

$$\begin{cases} lim_{i\to\infty} v_h(i) = v_{expect}(i) \\ lim_{i\to\infty} s_h(i) = s_{expect}(i) \end{cases} \tag{4}$$

where v_{expect} and s_{expect} are the expected speed and positon.

2) PLATOON STABILITY

The spacing error is expressed as follow:

$$\Delta d(i) = s_h(i) - s_{expect}(i) \tag{5}$$

The stability of the platoon can be described as:

$$max(\frac{\Delta d(i+1)}{\Delta d(i)}) \le 1 \tag{6}$$

B. BATTERY MODEL

The model of battery is established by the internal resistance equivalent model. The power of the battery P_{bat} is equal to the sum of the external power P_b and the depletion of internal resistance R. At the discharge state, the internal resistance is the discharge resistance R_{dis}. At the charge stage, the internal resistance is charging resistance R_{cha}. The open-circuit voltage U_{ocv} and the internal resistance R are both correlated with SOC.

$$P_{bat} = U_{ocv}(SOC) * I = I^2 * R(SOC) + P_b \tag{7}$$

The current can be solved by Equation (7) as follows:

$$I = \frac{U_{ocv} - \sqrt{U_{ocv}^2 - 4P_b * R(SOC)}}{2R(SOC)} \tag{8}$$

The changing rate of SOC can be expressed as follows:

$$\dot{SOC} = d(\frac{Q - \int_0^t Idt}{Q})/dt = -\frac{I}{Q} \tag{9}$$

where Q is the capacity of the battery.

C. BRAKING FORCE DISTRIBUTION MODEL

The braking force distribution model of the electric vehicle includes two parts. One part is the braking force distribution of the front and rear axle; the other part is the braking force distribution of the motor and hydraulic. The key point is to recycle as much braking energy as possible on the premise of meeting the braking safety. In this paper, the target vehicles are battery-electric vehicles driven by the front axle. The proposed strategy distributes more braking force to the front axle motor to get as much regenerative energy as possible. If it is necessary for high-intensity braking, the motor braking force should exit. Only the hydraulic system provides the braking force to prevent the wheel from locking and making full use of the ground adhesion conditions. To fully recycle the regenerative braking energy of every platoon member in the CACC mode, the braking force distribution strategy of a single EV is designed, as shown in Fig 1.

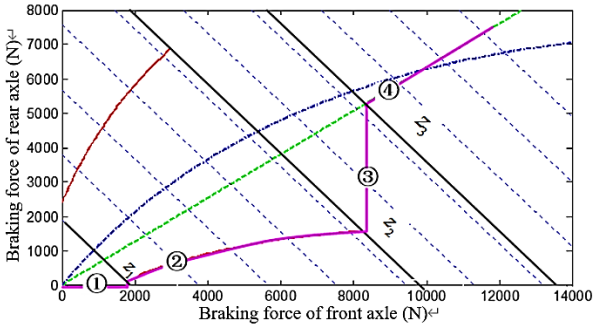

FIGURE 1. The braking force distribution strategy of CACC mode.

When braking strength $z < z_1$, there is no requirement for the braking force of the front axle in ECE regulation, and only the front axle motor provides the braking force; when the braking strength $z_1 < z < z_2$, the braking force of front and rear axles is distributed along the line of ECE regulation; when the braking strength $z_2 < z < z_3$, the motor brake force reaches the maximum, the braking force of the front axle remains unchanged, and the hydraulic braking force of the rear axle increases; when the braking strength $z > z_3$, the motor braking is abandoned, and the braking force is distributed along the β line to ensure safety and make full use of the ground adhesion characteristics. In the whole process of braking force distribution, if the motor braking force is insufficient, it is compensated by the hydraulic braking force. The distribution of the braking force is as follows.

$$\begin{cases} F_{bf} = F_b \\ F_{br} = 0 \quad (0 < z < z_1) \end{cases} \tag{10}$$

$$\begin{cases} \mathrm{F_{bf}} = \mathrm{F_b}\left(1 - \dfrac{(\mathrm{z}+0.04)(\mathrm{a}-\mathrm{zh_g})}{0.7\mathrm{zL}}\right) \\ \mathrm{F_{br}} = \mathrm{F_b}\dfrac{(\mathrm{z}+0.04)(\mathrm{a}-\mathrm{zh_g})}{0.7\mathrm{zL}} \quad (\mathrm{z_1 < z < z_2}) \end{cases} \tag{11}$$

$$\begin{cases} F_{bf} = \dfrac{T_{mot\_max} i_0}{r_w} \\ F_{br} = \dfrac{T_{mot\_max} i_0 (1 - \beta_{ECE-B})}{r_w \beta_{ECE-B}} \quad (z_2 < z < z_3) \end{cases} \tag{12}$$

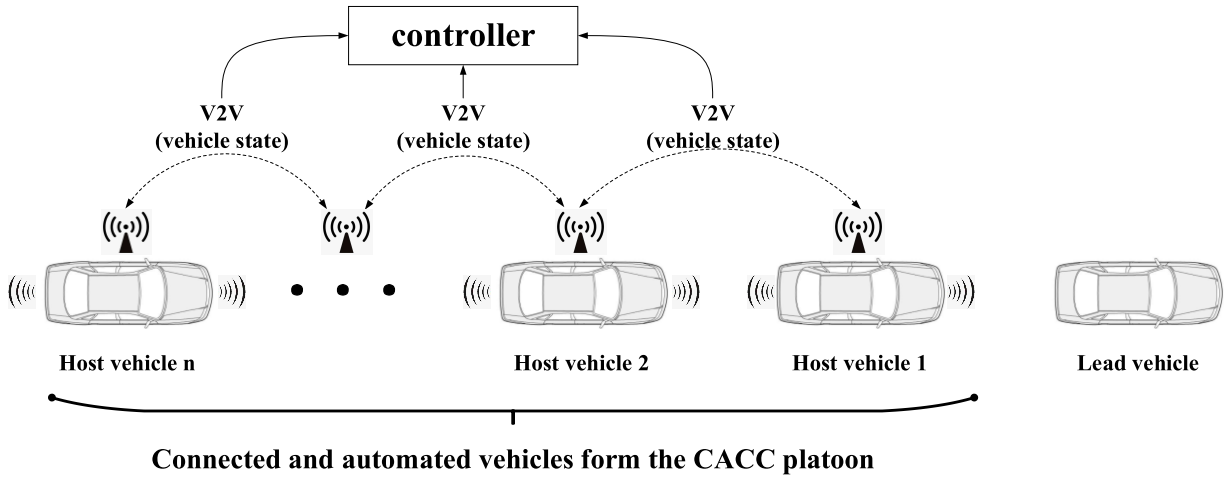

FIGURE 2. Diagram of the CACC system.

$$\begin{cases} F_{bf} = F_b\beta \\ F_{br} = F_b\,(1-\beta) \quad (z > z_3) \end{cases} \tag{13}$$

The boundary condition is

$$\begin{cases} z_1 = 0.1 \\ z_2 = \dfrac{-(b+0.04h_g)+\sqrt{(b-0.04h_g)^2+2.8T_{mot\_max}h_gL/r_wM}}{2h_gg} \\ z_3 = \left[\dfrac{1}{2h_g}\sqrt{b^2+\dfrac{4h_gLT_{mot\_max}}{Gr_w}}-\left(\dfrac{b}{h_g}+\dfrac{T_{mot\_max}}{r_w}\right)\right] \\ \quad +\dfrac{T_{mot\_max}}{Gr_w} \end{cases} \tag{14}$$

where F_{bf} and F_{br} are the braking force of front and rear axles of electric vehicles, F_b is the total demand braking force, h_g is the height of mass center, L is the total wheelbase, a, b are the front and rear wheelbase, T_{mot_max} is the maximum regenerative braking torque of the motor, i_0 is the speed ratio of the main reducer, r_w is the rolling radius of the wheel, β_{ECE-B} is the upper proportion of the braking force of the front axle to total braking force limited by ECE regulations. β is the proportion of the braking force of the front axle to the total braking force in the braking process. G is the weight of the vehicle, and g is the acceleration of gravity.

III. ALGORITHM

The structure of the CACC system is shown in Fig.2. The electric vehicle platoon is composed of n members from ''host vehicle 1'' to ''host vehicle n''. The adjacent host vehicles can transmit the vehicle state through wireless signals by the V2V technique. When a ''lead vehicle'' appears in front of the ''host vehicle 1'' in the same lane at an appropriate distance and the speed of the lead vehicle is lower than that of the platoon, the platoon should reduce the speed of every member and give a new cruising speed to accommodate the lead vehicle. This process is similar to the following mode of ACC. The control strategy model of this process is given in this section.

A. VEHICLE PLATOON FOLLOWING STRATEGY

The platoon spacing means the minimum safe distance between two adjacent vehicles in the platoon. If the spacing between two vehicles is less than the safe spacing, it is prone to cause collision or driver's panic. If the spacing between the two vehicles is much larger than the safe spacing, the platoon will be cut off easily. The vehicle spacing is the sum of two-part: the fixed spacing and variable spacing. Fixed spacing simply considers that the safe distance of two adjacent vehicles is fixed independent of vehicle speed and external environment. In this case, the fixed spacing is difficult to meet the actual needs. The safe distance in the variable spacing can be calculated by headway τ, vehicle speed v_h and the constant distance d_0, which meets the actual needs of drivers. The strategy of headway can be divided into fixed headway and variable headway. Fixed headway determines headway as a fixed value, which can be selected according to different drivers' driving habits. The variable headway strategy considers headway as a function of various driving state parameters.

The adaptive cruise system adopts the algorithm of variable vehicle spacing with fixed time headway.

$$d_{des}\,(v_h) = \tau v_h + d_0 \tag{15}$$

where $\tau = 1$, $d_0 = 20$.

B. VEHICLE PLATOON STATE PREDICTIVE CONTROL STRATEGY

The information transceiver module of all vehicles in the platoon shares the real-time information with the CACC controller through various sensors. The CACC controller calculates and transmits the desired longitudinal acceleration to the vehicle dynamics control module to realize the acceleration. Then the vehicle states information is updated and feeds back to the CACC controller. In the process of driving, the

vehicle dynamics controller orders the motor to output the expected torque. In vehicle braking, the vehicle dynamics controller distributes the motor braking force and hydraulic braking force according to the received control information. In this way, the closed-loop control is achieved; meanwhile, the performances of the electric vehicle should be taken into account in the control process.

According to the preset starting mode or the driver's pedal input at the starting process, the first vehicle in the electric vehicle platoon obtains the desired acceleration a_u. As the input of the model, there is a time delay from the expected acceleration a_u to the actual acceleration a_h of the vehicle system, and the transfer function of the control state equation is $a_h = Ka_u/(\tau s + 1)$. Where the parameter K is the gain, and τ is the time constant. These two parameters can be obtained by system identification and parameter calibration of the actual vehicle.

In this paper, the MPC algorithm is used to control the state of all vehicles in the platoon. The cost function and constraint conditions are set according to the predictive target to get the optimal solution of the model. The specific steps are as follows:

For the lead vehicle, only the current states are transmitted to the platoon through the sensor. The future states are unknown due to the driver. The future states should be predicted as the input of the MPC controller in the predictive horizon. Select the vehicle distance s_f, vehicle speed v_f, vehicle longitudinal acceleration a_f as the state variables x_f, i.e. $x_f = \begin{bmatrix} s_f & v_f & a_f \end{bmatrix}^T$. The discrete state-space equation can be expressed as follows in the predictive horizon:

$$x_f\,(i+1) = A_f x_f\,(i) \tag{16}$$

$$A_f = \begin{bmatrix} 1 & T_s & T_s^2/2 \\ 0 & 1 & T_s \\ 0 & 0 & 1 \end{bmatrix} \tag{17}$$

Let A_f denote the state parameter coefficient matrix. The general formula to use the states of the current vehicle $x_f(i)$ to forecast the states $x_f(i+k)$ at the time $i+k$ is

$$x_f\,(i+k) = A_f^k x_f\,(i) \tag{18}$$

The host vehicles share their information with each other. The states of lead vehicle and host vehicles are known to the host vehicles. Hence, the states are used as input to the MPC controller. The MPC controller outputs the control variables to host vehicles keeping the characteristics of the platoon.

For the first vehicle (subscript 1) in the platoon. Select the vehicle distance $s_{h(1)}$, vehicle speed $v_{h(1)}$, vehicle longitudinal acceleration $a_{h(1)}$ and change rate of longitudinal acceleration $j_{(1)}$ as the state variables $x_{h(1)}$, i.e. $x_{h(1)} = \begin{bmatrix} s_{h(1)} & v_{h(1)} & a_{h(1)} & j_{(1)} \end{bmatrix}^T$, take the expected acceleration of this vehicle $a_{u(1)}$ as control variable $u_{(1)}$. i represents the marked value at every sampling time. The discrete state-space equation can be expressed as follows:

$$x_{h(1)}(i+1) = A'_{(1)}x_{h(1)}(i) + B'_{(1)}u_{(1)}(i) \tag{19}$$

$$A'_{(1)} = \begin{bmatrix} 1 & T_s & T_s^2/2 & 0 \\ 0 & 1 & T_s & 0 \\ 0 & 0 & 1 - T_s/\tau & 0 \\ 0 & 0 & -1/\tau & 0 \end{bmatrix} \tag{20}$$

$$B'_{(1)} = \begin{bmatrix} 0 \\ 0 \\ T_s K/\tau \\ K/\tau \end{bmatrix} \tag{21}$$

$$u_{(1)} = a_{u(1)} \tag{22}$$

The first vehicle of the platoon needs to achieve the objection to follow the front vehicle. Due to that, the movement of the front vehicle is uncertain; the parameters in the state space function of the first vehicle should be set as many as possible to predict the vehicle state precisely. The initial state is known from the second vehicle to the last vehicle in the electric vehicle platoon to simplify the state space function.

The state vector could be simplified from the second vehicle to the last vehicle in the platoon. Select vehicle distance $s_{h(n)}$, vehicle speed $v_{h(n)}$, vehicle longitudinal acceleration $a_{h(n)}$ as state variable $x_{h(n)}$, i.e. $x_{h(n)} = \begin{bmatrix} s_{h(n)} & v_{h(n)} & a_{h(n)} \end{bmatrix}^T$, expected acceleration of the vehicle $a_{u(n)}$ as control variable $u_{(n)}$, i as the marked value at every sampling time. The discrete state-space equation can be expressed as follows:

$$x_{h(n)}(i+1) = A'_{(2)}x_{h(n)}(i) + B'_{(2)}u_{(n)}(i) \tag{23}$$

$$A'_{(2)} = \begin{bmatrix} 1 & T_s & T_s^2/2 \\ 0 & 1 & T_s \\ 0 & 0 & 1 - T_s/\tau \end{bmatrix} \tag{24}$$

$$B'_{(2)} = \begin{bmatrix} 0 \\ 0 \\ T_s K/\tau \end{bmatrix} \tag{25}$$

$$u_{(n)} = a_{u(n)} \tag{26}$$

The discrete state-space equation of the rear vehicles is the same as that of the second vehicle.

Let A denote the state parameter coefficient matrix, B denote the input parameter coefficient matrix, u denote the input parameter, and the subscript n denote the nth electric vehicle in the platoon. Then the general formula to use the states of the current vehicle $x_{(n)}(i)$ to forecast the states at the time $i+1$ $x_{(n)}(i+1)$ is

$$x_{(n)}\,(i+1) = A_{(n)}x_{(n)}\,(i) + B_{(n)}u_{(n)} \tag{27}$$

The general formula to use the states of current vehicle $x_{(n)}(i)$ to forecast the states after k intervals $x_{(n)}(i+k)$ is

$$x_{(n)}\,(i+k) = A_{(n)}^k x_{(n)}\,(i) + \begin{bmatrix} A_{(n)}^{k-1} & A_{(n)}^{k-2} & \cdots & A_{(n)} & I \end{bmatrix} \times B_{(n)} \begin{bmatrix} u_{(n)}(i) \\ u_{(n)}(i+1) \\ \cdots \\ u_{(n)}(i+k-1) \end{bmatrix} \tag{28}$$

where $x_{(n)}(i)$ is the *n-th* vehicle state vector at the time i, $x_{(n)}(i+1)$ is the *n-th* vehicle state vector at the time $(i+1)$, and $x_{(n)}(i+k)$ is the *n-th* vehicle state vector after k intervals.

When $n = 1, A_{(1)} = A'_{(1)}, B_{(1)} = B'_{(1)}$; otherwise $A_{(n)} = A'_{(2)}$, $B_{(n)} = B'_{(2)}$.

For a specific vehicle in the platoon, the initial state is known. The states in the next predictive horizon can be predicted according to equation (19) - (28). The corresponding optimal control can be carried out according to the prediction results. The next time, according to the same prediction method, the predictive horizon can be pushed back one time-step, and this step will run continuously. The prediction model can output the vehicle state at any time in the future predictive horizon.

C. ESTABLISHMENT OF OBJECTIVE FUNCTION AND CONSTRAINT

According to the above method, the moving distance, speed, and acceleration of all platoon vehicles are obtained in the predictive horizon. For the adjacent vehicles in the platoon, the adaptive cruise objective function can be designed according to the kinematic parameters in state vectors. For the platoon composed of N electric vehicles, a set of $(N-1)$ corresponding objective functions can be created, which can be weighted to get the overall objective function of the platoon.

The objective function includes three indices: the following performance index, the comfortability index, and the economy index. k is the sequence number of a specific time interval in the predictive horizon.

The following performance index of the platoon l_{track}, including vehicle spacing and vehicle speed, is calculated by

$$l'_{track(n)}(k) = w_d(\Delta d(k))^2 + w_v(\Delta v(k))^2 \quad (29)$$

$$\Delta d(k) = s_{(n-1)}(k) - s_{(n)}(k) - d_{des}\left(v_{(n)}(k)\right) \quad (30)$$

$$\Delta v(k) = v_{(n)}(k) - v_{(n-1)}(k) \quad (31)$$

$$l_{track} = \sum_{n=2}^{N}\sum_{k=1}^{P} l'_{track(n)}(k) \quad (32)$$

where $l'_{track(n)}(k)$ is the following performance index at the time k; $\Delta d(k)$ is the distance error between two vehicles at the time k; $\Delta v(k)$ is the speed error between two vehicles at the time k; $s_{(n-1)}(k)$ and $s_{(n)}(k)$ is the driving distance of the front car and the rear car at the time k, which is given by the model prediction algorithm; $v_{(n)}(k)$ and $v_{(n-1)}(k)$ is the driving speed of the rear car and the front car at the time k, which is given by the model prediction algorithm; $d_{des}\left(v_{(n)}(k)\right)$ is the expected spacing corresponding to rear vehicle speed $v_{(n)}(k)$, i.e. $d_{des}\left(v_{(n)}(k)\right) = \tau v_{(n)}(k) + d_0$; w_d is the weight of distance error and w_v is the weight of vehicle speed error in the total objective function.

The vehicle comfortability index is $l_{confort}$ including vehicle acceleration and acceleration change rate. The calculation formula is

$$l'_{confort(n)}(k) = w_c(a_{(n)}(k))^2 + w_j[(a_{(n)}(k) - a_{(n)}(k-1))]^2 \quad (33)$$

$$l_{confort} = \sum_{n=1}^{N}\sum_{k=1}^{P} l'_{confort(n)}(k) \quad (34)$$

where $l_{cofort(n)}{}'(k)$ is the comfortability index value at the time k; $a_{(n)}(k)$ and $a_{(n)}(k-1)$ is the acceleration value of a platoon member at the time k and $k-1$; w_c and w_j are the weight of the acceleration and acceleration change rate of the vehicle in the total objective function.

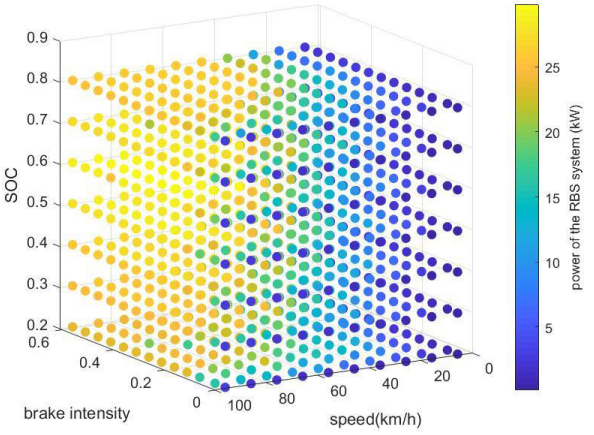

FIGURE 3. The look-up table of the RBS system.

$l_{economy}$ is the vehicle economy index, including the regenerated energy of the vehicle braking process. The calculation principle is:

$P(v_{(n)}(k), z\left(a_{(n)}(k)\right), SOC(k-1))$ is the power recycled by the RBS system when a platoon member brake in a specific time interval, which is determined according to looking up the table by the vehicle's speed $v_{(n)}(k)$, braking intensity $z\left(a_{(n)}(k)\right)$ at the time k and SOC of the previous moment $SOC(k-1)$. Braking intensity $z\left(a_{(n)}(k)\right)$ is

$$z\left(a_{(n)}(k)\right) = a_{(n)}(k)/g \quad (35)$$

SOC is a continuously changing value. $SOC(k)$ is calculated by $SOC(k-1)$ at the last moment. Firstly, interpolate the charge and discharge voltage $uchg(k)$ of the battery at the time k according to $SOC(k-1)$. Secondly, interpolate the charge and discharge power $Pbat(k)$ of the battery at the time k according to $SOC(k-1)$, $z\left(a_{(n)}(k)\right)$ and $v_{(n)}(k)$ as shown in Fig.3; $Pbat(k)/uchg(k)$ is the charge and discharge current at the time k. The change of SOC is calculated by the current value, sampling time, and total capacity of the battery; thus, the SOC at the time k can be obtained:

$$SOC(k) = SOC(k-1) + \frac{Pbat(k)}{uchg(k)} * T_s/(3600Q) \quad (36)$$

where T_s is the length of the time interval.

where w_e is the weight of the economy index in the total objective function, $l'_{economy(n)}(k)$ is the economy index value at the time k, then

$$l'_{economy(n)}(k) = w_e\left[P(v_{(n)}(k), z\left(a_{(n)}(k)\right), SOC(k-1)\right]T_s \quad (37)$$

$$l_{economy} = \sum_{n=1}^{N}\sum_{k=1}^{P} l'_{economy(n)}(k) \quad (38)$$

The objective function is the sum of the three indices:

$$l = l_{track} + l_{confort} + l_{economy} \quad (39)$$

Constraint: Restraint range of distance error between the front and rear vehicles

$$\Delta d_{min} \leq d_{(n-1)}(k) - d_{(n)}(k) - d_{des}(v_{(n)}(k)) \leq \Delta d_{max} \quad (40)$$

where $d_{(n-1)}(k)$ and $d_{(n)}(k)$ are the distance driven by the front vehicle and the rear vehicle at the time k; $d_{des}(v_{(n)}(k))$ is the ideal spacing according to the rear vehicle speed $v_{(n)}(k)$; Δd_{min} and Δd_{max} is the lower and upper limit of the allowable range of the distance error between two adjacent vehicles in the platoon.

Restriction range of speed difference between two adjacent vehicles

$$\Delta v_{min} \leq v_{(n)}(k) - v_{(n-1)}(k) \leq \Delta v_{max} \quad (41)$$

where $v_{(n)}(k)$ and $v_{(n-1)}(k)$ is the speed of the rear and front vehicle at the time k; Δv_{min} and Δv_{max} is the lower and upper limit of the allowable range of vehicle speed error for adjacent vehicles in the platoon.

Acceleration constraint of a single-vehicle

$$a_{min} \leq a_{(n)}(k) \leq a_{max} \quad (42)$$

where $a_{(n)}(k)$ is the acceleration value of a single-vehicle at the time k; a_{min} and a_{max} is the maximum deceleration and acceleration of a single-vehicle.

Single vehicle acceleration variation constraint

$$\Delta a_{min} \leq (a_{(n)}(k) - a_{(n)}(k-1))/T_s \leq \Delta a_{max} \quad (43)$$

where $a(k)$ and $a(k-1)$ are the acceleration of a single-vehicle at the time k and $k-1$; Δa_{min} and Δa_{max} is the lower and upper limit of the acceleration variation.

The constraint can be written as penalty function C:

$$C_{(n)}(k) = \begin{cases} 0 & if\ meet\ the\ constraint \\ +\infty, & otherwise \end{cases} \quad (44)$$

$$C(k) = \sum_{n=1}^{N} C_{(n)}(k) \quad (45)$$

D. OBJECTIVE FUNCTION SOLUTION

It is necessary to use the look-up table to obtain the regenerative braking power under the current speed and braking intensity for the economy index, a nonlinear discontinuous objective value in the objective function. It is difficult to use the conventional quadratic programming algorithm to solve it. In this case, the heuristic algorithm can solve the problem according to the probability method. This paper uses the simulated annealing and particle swarm optimization algorithm (SA-PSO) to solve the objective function. Steps are as follows:

Step 1. Initialize every particle parameter. The acceleration value of every vehicle in the platoon constitute a particle population $p_1 = \{a_1, a_2, \ldots, a_N\}$, population size N equals the number of platoon members. Random update factor c_1, annealing rate λ, the maximum number of iterations i_{max} and the minimum fitness value d_{stop} are set during initialization, where d_{stop} is set to a large constant;

Step 2. Set the fitness function. Take the objective function as a part of the fitness function; another factor is the constraint set as penalty function $C(k)$. Calculate and record the fitness value of the initialized particle under the fitness function, and d_{stop} equals to this fitness value, the corresponding particle population is recorded as p_g. The fitness function J is

$$J(k) = \sum_{n=2}^{N} l'_{track}(k) + \sum_{n=1}^{N} (l'_{confort}(k) + l'_{economy}(k) + C(k)) \quad (46)$$

$$J = l_{track} + l_{confort} + l_{economy} = \sum_{k=1}^{P} J(k) \quad (47)$$

$$d_{stop} = min\, J \quad (48)$$

Step3. Determine the initial temperature $t_0 = \mathrm{d_{stop}}$;

Step4. Use random update factor c_1, acceleration range and population $p_g(i)$ to get a new set of the particle population $p_g(i+1)$, and i self-increasing 1, until reach i_{max}:

$$p_g(i+1) = p_g(i) + c_1[a_{min}, a_{max}]_N \quad (49)$$

Step5. Record the adaptation value d_{temp} at the current temperature, if $d_{temp} \leq d_{stop}$, then accept and equal p_g to the population set p_f corresponding to d_{temp}. If $d_{temp} > d_{stop}$, then accept $p_f = p_g(i+1)$ with the probability $\exp[-\frac{d_{temp}-d_{stop}}{t}]$, or accept p_g unchanged with the probability $(1 - \exp\left[-\frac{d_{temp}-d_{stop}}{t}\right])$, i.e

$$P\{p_f = p_g(i+1)\} = exp[-\frac{d_{temp} - d_{stop}}{t}] \quad (50)$$

$$P\{p_f = p_g(i)\} = 1 - exp[-\frac{d_{temp} - d_{stop}}{t}] \quad (51)$$

Step 6. Return to step 4 until i reach i_{max}, then given $i = 1$ and $p_g(i) = p_f$.

Step 7. Conduct cooling operation ($t_{k+1} = \lambda t_k$);

Step 8. Cooldown and return to step 4 until the minimum temperature is reached, and output the particle and optimal global value at this time.

IV. SIMULATION

The CACC strategy proposed in this article is compared with the CACC and ACC strategy by simulation. The CACC control strategy is embedded in Matlab / Simulink as S-function. The vehicle kinematics model of the platoon composed of four electric vehicles is established for simulation in Simulink. All vehicle in the platoon correspond to the same parameters, and the setting parameters are as shown in Table 1 and Table 2:

Fig.6 and Fig.7 are the longitudinal cruise speed and acceleration graphs of the platoon composed of four electric vehicles in the CACC mode with the economy index. Fig.8 and Fig.9 are graphs of the longitudinal cruise speed and acceleration of the same platoon in the CACC mode without the economy index. Fig.10 is the graph of cruise speed and acceleration of the platoon without internal communication.

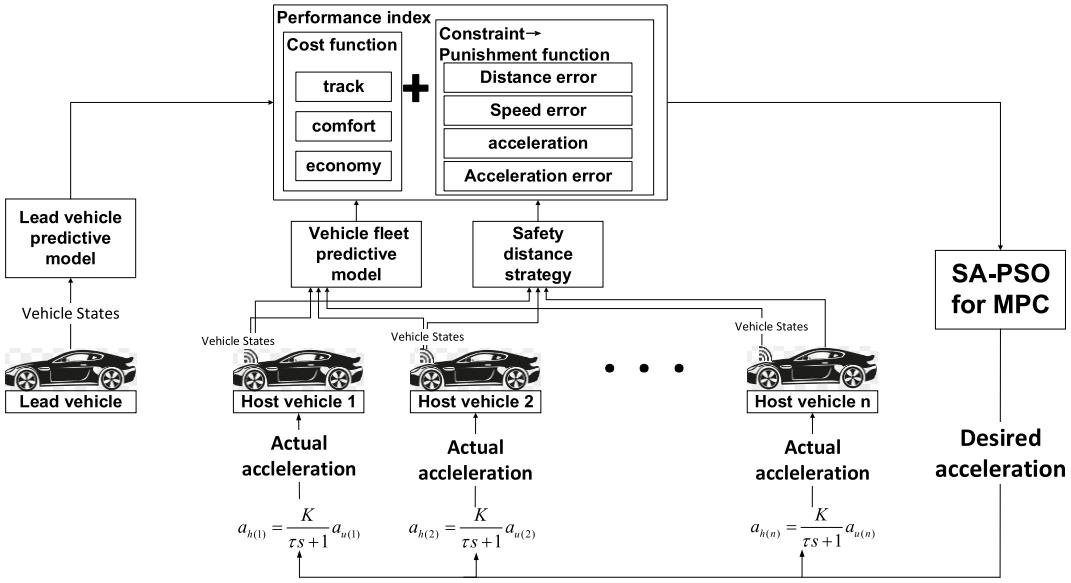

FIGURE 4. The overall diagram of vehicle platoon CACC strategy.

TABLE 1. Vehicle parameter setting.

Vehicle parameter	Symbol	Value	Unit
Curb quality	m	1800	kg
Wheelbase	L	2800	mm
Centroid height	h_g	0.5	m
Front wheelbase	a	1200	mm
Rear wheelbase	b	1600	mm
Air resistance coefficient	C_D	0.3	
Frontal area	A	1.4	m^2
Rolling resistance coefficient	f	0.015	
Wheel rolling radius	r_w	0.307	m
Maximum power of the motor	P_{max}	60	kW
Maximum braking torque of the motor	T_{mot_max}	20	Nm
Battery capacity	Q	60	Ah

TABLE 2. Model parameter setting.

Model parameter	Symbol	Value	Unit
Sampling time	T_s	0.05	s
Prediction time domain	P	1.8	s
Spacing error weight	w_d	10	
Speed error weight	w_v	10	
Expected acceleration weight	w_a	5	
Acceleration rate weight	w_j	2	
Energy recovery weight	w_e	-10	
Maximum spacing	Δd_{max}	20	m
Minimum spacing	Δd_{min}	0	m
Maximum speed error	Δv_{max}	5	m/s
Minimum speed error	Δv_{min}	-5	m/s
Maximum expected acceleration	a_{max}	6	m/s^2
Minimum expected acceleration	a_{min}	-8	m/s^2
The upper limit of acceleration change	Δa_{max}	5	m/s^2
The lower limit of acceleration change	Δa_{min}	-5	m/s^2

TABLE 3. SA-PSO parameter setting.

Model parameter	Symbol	Value	Unit
Random update factor	c_1	0.2	
maximum number of iterations	c_2	150	
population size	N	20	
minimum fitness initial value	t_0	2000	
annealing rate	λ	0.96	

Comparing the speed graphs in the three cases of Fig.6, Fig.8, and Fig.10, the result shows that the following performance of the CACC mode on vehicle speed is better than the ACC mode: the speed of the CACC mode with economy index and the CACC mode without economy index do not appear overshoot, and the following performs well, and the safety of the platoon is achieved; however, in the ACC mode, the apparent overshoot and response delay of the speed will cause the spacing fluctuation between the vehicles in the platoon. If acceleration and deceleration frequently change during the process, the driving spacing tends to be dangerous, and the stability will worsen.

Comparing the acceleration graphs in Fig. 7, Fig. 9, and Fig. 11, the CACC with economy index mode uses a heuristic algorithm as an optimization strategy, which directly outputs the vehicle acceleration. The acceleration has a certain degree of fluctuation in CACC mode with the economy index. It means that the comfortability of the vehicle in this mode is worse than that in CACC mode without the economy

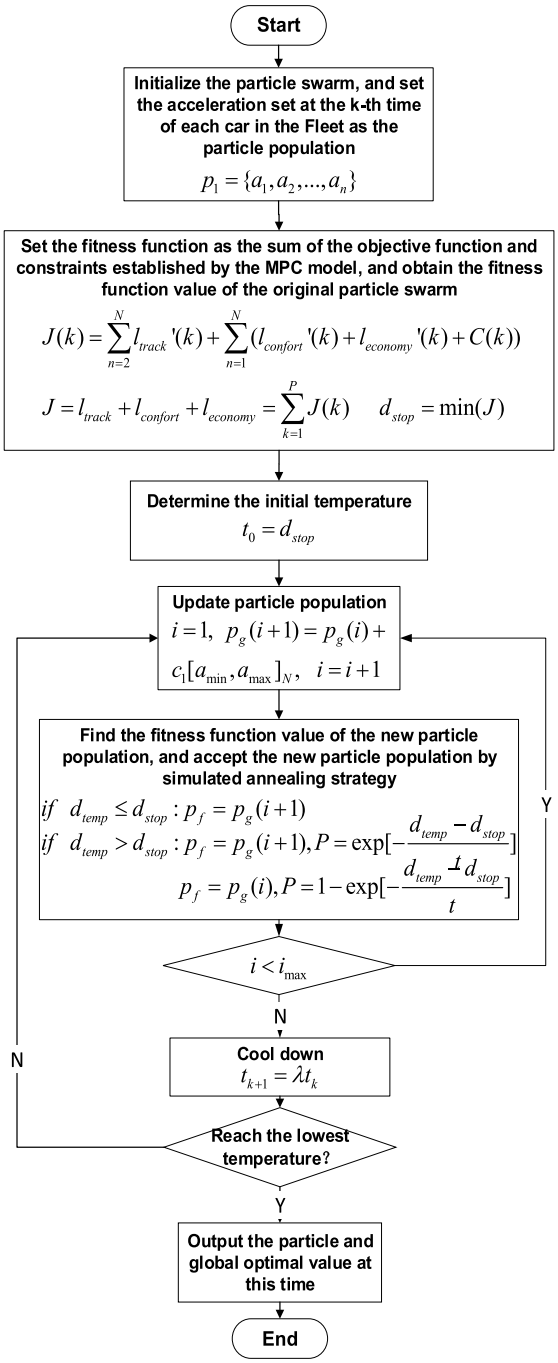

FIGURE 5. Flow chart of SA-PSO algorithm.

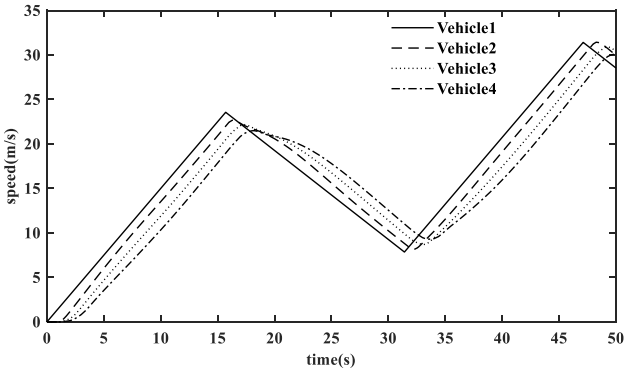

FIGURE 6. Speed profile under CACC with economy index.

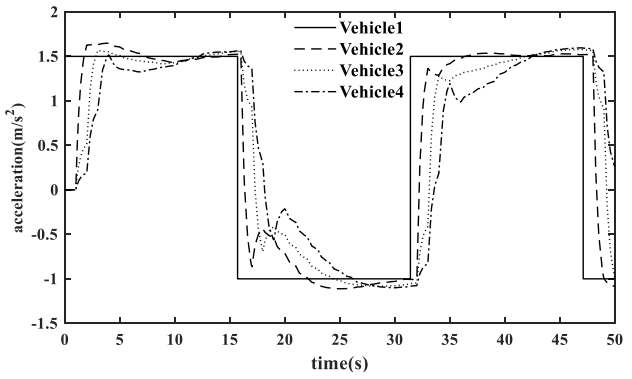

FIGURE 7. Acceleration profile under CACC with economy index.

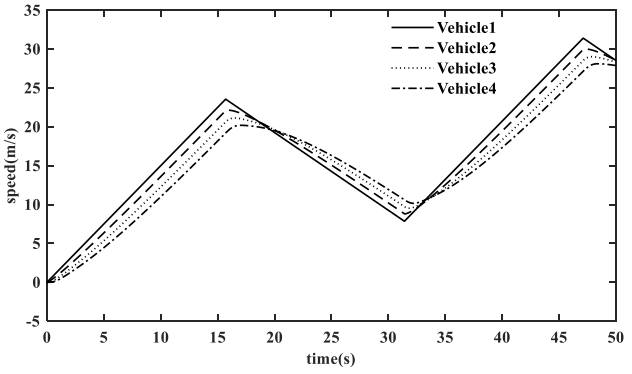

FIGURE 8. Speed profile under CACC without economy index.

index. The overshoot is the product that the rear vehicles control the acceleration to satisfy the safe spacing and speed error brought by the speed ahead of vehicle 1. However, the economy of the vehicle is improved, which is obtained in the following simulation results; The CACC mode without economy index has better stability in acceleration and has no overshoot and little response delay in meeting the comfortability. While in the ACC mode, there are clear overshoots and response delay in acceleration. The ACC mode has the worst performance. As the number of vehicles increasing in the platoon, the acceleration of the rear vehicle becomes more extensive, and the platoon shows evident overshoot and response delay. Once the ACC strategy receives slight disturbances during the multi-vehicle following process, the subsequent platoon is prone to oscillations; the stability is not guaranteed. The overshoots and response delay can be regarded as instability, which brings discomfort to drivers.

Fig.11 and Fig.12 are graphs of the speed and acceleration of the platoon using the CACC strategy in NEDC. Vehicle 2-4 only have a little time delay on driving away compared with Vehicle 1. The reason is that the states of

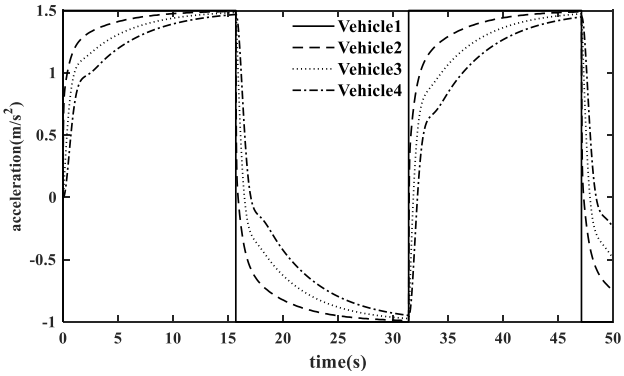

FIGURE 9. Acceleration profile under CACC without economy index.

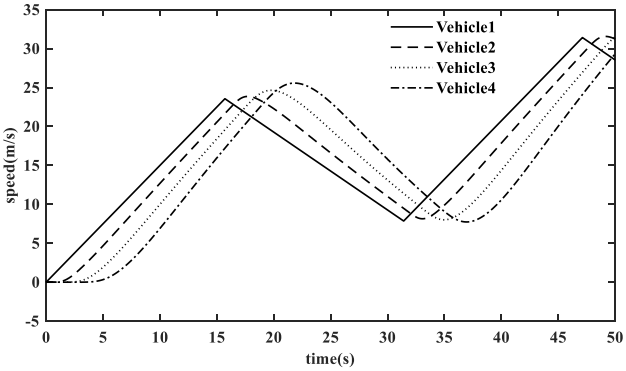

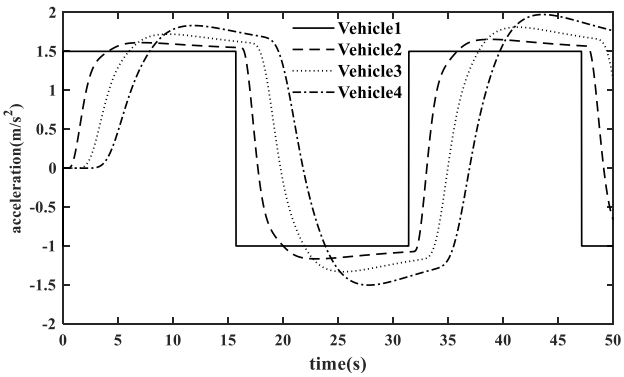

FIGURE 10. Speed & acceleration profile under ACC without platoon communication.

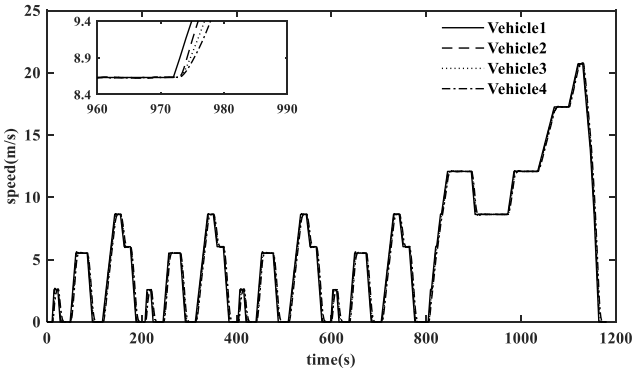

FIGURE 11. NEDC cycle speed profile under CACC with economy index.

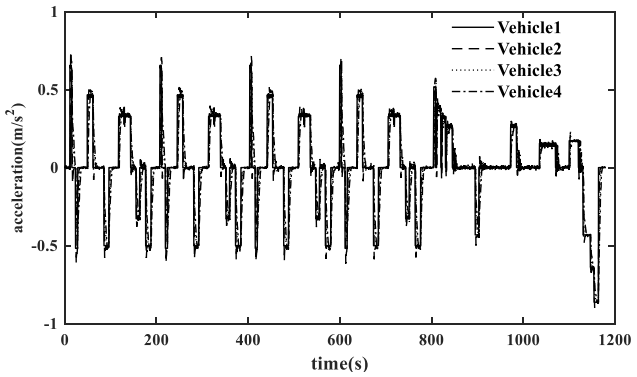

FIGURE 12. NEDC cycle acceleration profile under CACC with economy index.

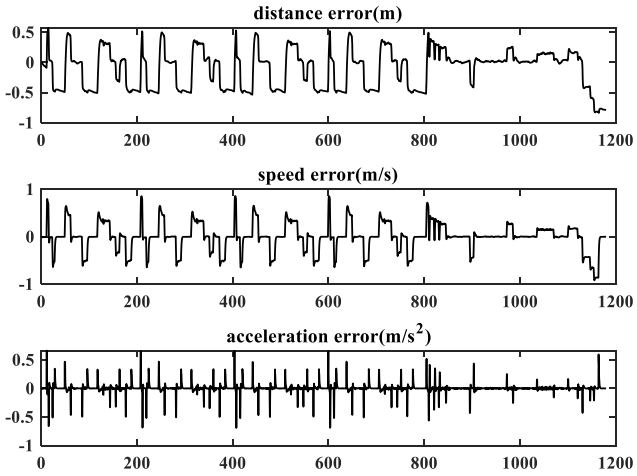

FIGURE 13. Spacing, speed, and acceleration error of vehicle 1 and vehicle 2 in the NEDC cycle under CACC with economy index.

vehicle 1 could not be accurately predicted when the states of vehicle 1 undergoes a sudden change, which leads a response delay to host vehicles. Overall, Vehicle 2-4 perform well. It can result from Fig. 11 and Fig. 12 that the CACC strategy shows strong following performance, stability characteristics and completes the driving cycle without risk in a complete driving cycle. Figure 13-15 are graphs of the change of the distance, speed, and acceleration error between two adjacent vehicles. It can be found that the error in Figure 13 is bigger than Figure 14-15. The acceleration of vehicle 2-4 is planned to achieve the performances at the same time. As a platoon, the performances are well evaluated to reduce the error. The speed of vehicle 1 is independent of vehicle 2-4, which leads to a forecast bias. The forecast bias is the reason of error. Figure 13-15 show that the distance, speed error, and acceleration error between two adjacent vehicles are controlled within a reasonable range. The CACC strategy completes the driving task well since the vehicle spacing error is one of the optimization objectives.

Table 4 shows that the economic efficiency of the CACC strategy is 8.5% higher than that of the ACC strategy; the

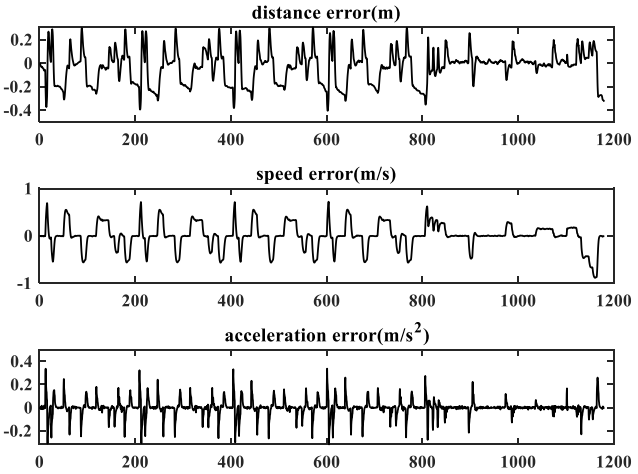

FIGURE 14. Spacing, speed, and acceleration error of vehicle 2 and vehicle 3 in the NEDC cycle under CACC with economy index.

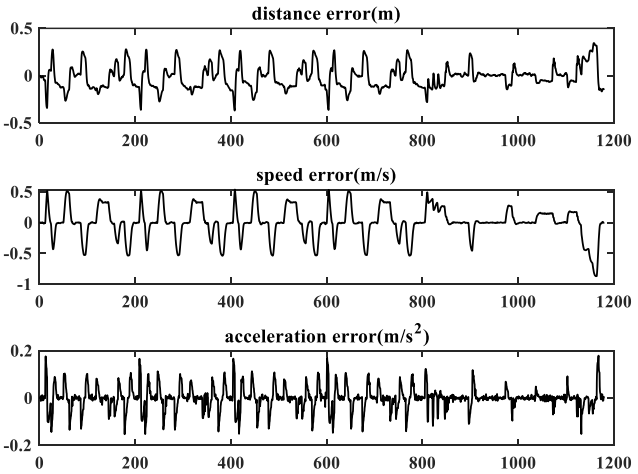

FIGURE 15. Spacing, speed, and acceleration error of vehicle 3 and vehicle 4 in the NEDC cycle under CACC with economy index.

TABLE 4. Comparison of economic indicators in NEDC.

	CACC with economy index	CACC without economy index	ACC
Total recycled braking energy	0.141kWh	0.130kWh	0.121kWh

economic efficiency of the CACC strategy with the economy index is 16.5% higher than that of the ACC strategy in NEDC. In the CACC strategy without economy index, considering the comfortability, safety, and following performance indices, the max vehicle spacing error is 3.6% in NEDC. When the economy index is added to the objective function, the vehicle spacing error slightly expands. The reason is that after adding a new economy index into the multi-objective optimization function, the following index is relatively weakened; meanwhile, the ability to control the spacing of the platoon is weakened. It is the contradiction between economy and other characteristics. It can be optimized by adjusting the weights, which is also the idea that can be expanded by subsequent research.

V. CONCLUSION

In this paper, an MPC controller based on the SA-PSO algorithm is proposed for the CACC system of electric vehicles. The MPC controller with the SA-PSO algorithm solves the optimization problem of nonlinear multi-objective effectively. In the simulation, the CACC algorithm uses a platoon formed by four electric vehicles to compare the result with the ACC strategy. The results show that the CACC strategy maintains the distance better between the adjacent vehicles and reduces the spacing to meet the adaptive cruise demand of the platoon. And the acceleration and speed of the CACC strategy perform a quick response with little overshoot and time delay. In the aspect of the economy, compared with the ACC strategy, the CACC strategy improves the overall regenerative braking energy of the platoon by about 16.5% in NEDC; it brings more economic benefits to drivers. The CACC strategy proposed in this paper improves the following performance, economy of the platoon and ensures the safety and comfortability of the vehicle as well. However, with the adding of economy index, there is a little vibration in the acceleration. The weight of multiple optimization objectives could be further optimized to balance the contradiction between comfortability and economy.

Future work should focus on the theoretical optimization of the ideal distance between platoon members and the modeling differences of individual vehicles in the platoon.

REFERENCES

[1] I. Mahdinia, R. Arvin, A. J. Khattak, and A. Ghiasi, "Safety, energy, and emissions impacts of adaptive cruise control and cooperative adaptive cruise control," *Transp. Res. Rec., J. Transp. Res. Board*, vol. 2674, no. 6, pp. 253–267, May 2020.

[2] Y. He, Q. Zhou, M. Makridis, K. Mattas, J. Li, H. Williams, and H. Xu, "Multiobjective co-optimization of cooperative adaptive cruise control and energy management strategy for PHEVs," *IEEE Trans. Transport. Electrific.*, vol. 6, no. 1, pp. 346–355, Mar. 2020.

[3] Q. Wang, X. Yang, Z. Huang, and Y. Yuan, "Multi-vehicle trajectory design during cooperative adaptive cruise control platoon formation," *Transp. Res. Rec., J. Transp. Res. Board*, vol. 2674, no. 4, pp. 30–41, Apr. 2020.

[4] C. Wang, Y. Dai, and J. Xia, "A CAV platoon control method for isolated intersections: Guaranteed feasible multi-objective approach with priority," *Energies*, vol. 13, no. 3, p. 625, Feb. 2020.

[5] B. Goñi-Ros, W. J. Schakel, A. E. Papacharalampous, M. Wang, V. L. Knoop, I. Sakata, B. van Arem, and S. P. Hoogendoorn, "Using advanced adaptive cruise control systems to reduce congestion at sags: An evaluation based on microscopic traffic simulation," *Transp. Res. Part C, Emerg. Technol.*, vol. 102, pp. 411–426, May 2019.

[6] A. Spiliopoulou, D. Manolis, F. Vandorou, and M. Papageorgiou, "Adaptive cruise control operation for improved motorway traffic flow," *Transp. Res. Rec., J. Transp. Res. Board*, vol. 2672, no. 22, pp. 24–35, Dec. 2018.

[7] Z. Haroon, B. Khan, U. Farid, S. M. Ali, and C. A. Mehmood, "Switching control paradigms for adaptive cruise control system with stop- and-go scenario," *Arabian J. Sci. Eng.*, vol. 44, no. 3, pp. 2103–2113, Mar. 2019.

[8] M. M. Brugnolli, B. A. Angelico, and A. A. M. Lagana, "Predictive adaptive cruise control using a customized ECU," *IEEE Access*, vol. 7, pp. 55305–55317, 2019.

[9] A. Weißmann, D. Görges, and X. Lin, "Energy-optimal adaptive cruise control combining model predictive control and dynamic programming," *Control Eng. Pract.*, vol. 72, pp. 125–137, Mar. 2018.
[10] S. Zhang and X. Zhuan, "Study on adaptive cruise control strategy for battery electric vehicle," *Math. Problems Eng.*, vol. 2019, pp. 1–14, Dec. 2019.
[11] P. Shakouri and A. Ordys, "Nonlinear model predictive control approach in design of adaptive cruise control with automated switching to cruise control," *Control Eng. Pract.*, vol. 26, pp. 160–177, May 2014.
[12] S. Li, K. Li, R. Rajamani, and J. Wang, "Model predictive multi-objective vehicular adaptive cruise control," *IEEE Trans. Control Syst. Technol.*, vol. 19, no. 3, pp. 556–566, May 2011.
[13] Y. Wu, B. Jiang, and N. Lu, "A descriptor system approach for estimation of incipient faults with application to high-speed railway traction devices," *IEEE Trans. Syst., Man, Cybern. Syst.*, vol. 49, no. 10, pp. 2108–2118, Oct. 2019.
[14] Y. Wu, B. Jiang, and Y. Wang, "Incipient winding fault detection and diagnosis for squirrel-cage induction motors equipped on CRH trains," *ISA Trans.*, vol. 99, pp. 488–495, Apr. 2020.
[15] J.-N. Meier, A. Kailas, O. Abuchaar, M. Abubakr, R. Adla, M. Ali, G. Bitar, R. Deering, U. Ibrahim, P. Kelkar, V. V. Kumar, E. Moradi-Pari, J. Parikh, S. Rajab, M. Sakakida, and M. Yamamoto, "On augmenting adaptive cruise control systems with vehicular communication for smoother automated following," *Transp. Res. Rec., J. Transp. Res. Board*, vol. 2672, no. 22, pp. 67–77, Dec. 2018.
[16] M. A. S. Kamal, M. Mukai, J. Murata, and T. Kawabe, "Ecological vehicle control on roads with up-down slopes," *IEEE Trans. Intell. Transp. Syst.*, vol. 12, no. 3, pp. 783–794, Sep. 2011.
[17] C. L. Melson, M. W. Levin, B. E. Hammit, and S. D. Boyles, "Dynamic traffic assignment of cooperative adaptive cruise control," *Transp. Res. Part C, Emerg. Technol.*, vol. 90, pp. 114–133, May 2018.
[18] K. Lidstrom, K. Sjoberg, U. Holmberg, J. Andersson, F. Bergh, M. Bjade, and S. Mak, "A modular CACC system integration and design," *IEEE Trans. Intell. Transp. Syst.*, vol. 13, no. 3, pp. 1050–1061, Sep. 2012.
[19] Y. Liu and B. Xu, "Improved protocols and stability analysis for multivehicle cooperative autonomous systems," *IEEE Trans. Intell. Transp. Syst.*, vol. 16, no. 5, pp. 2700–2710, Oct. 2015.
[20] R. A. Shet and F. Schewe, "Performance evaluation of cruise controls and their impact on passenger comfort in autonomous vehicle platoons," in *Proc. IEEE 89th Veh. Technol. Conf.*, Apr./May 2019, pp. 244–262.
[21] Y. Li, C. Xu, L. Xing, and W. Wang, "Integrated cooperative adaptive cruise and variable speed limit controls for reducing rear-end collision risks near freeway bottlenecks based on micro-simulations," *IEEE Trans. Intell. Transp. Syst.*, vol. 18, no. 11, pp. 3157–3167, Nov. 2017.
[22] Y. Zhu, D. Zhao, and Z. Zhong, "Adaptive optimal control of heterogeneous CACC system with uncertain dynamics," *IEEE Trans. Control Syst. Technol.*, vol. 27, no. 4, pp. 1772–1779, Jul. 2019.
[23] B.-J. Chang, R.-H. Hwang, Y.-L. Tsai, B.-H. Yu, and Y.-H. Liang, "Cooperative adaptive driving for platooning autonomous self driving based on edge computing," *Int. J. Appl. Math. Comput. Sci.*, vol. 29, no. 2, pp. 213–225, Jun. 2019.
[24] V. Milanes, S. E. Shladover, J. Spring, C. Nowakowski, H. Kawazoe, and M. Nakamura, "Cooperative adaptive cruise control in real traffic situations," *IEEE Trans. Intell. Transp. Syst.*, vol. 15, no. 1, pp. 296–305, Feb. 2014.
[25] B. van Arem, C. J. G. van Driel, and R. Visser, "The impact of cooperative adaptive cruise control on traffic-flow characteristics," *IEEE Trans. Intell. Transp. Syst.*, vol. 7, no. 4, pp. 429–436, Dec. 2006.
[26] M. H. Almannaa *et al.*, "Field implementation and testing of an automated eco-cooperative adaptive cruise control system in the vicinity of signalized intersections," *Transp. Res. D, Transp. Environ.*, vol. 67, pp. 244–262, Feb. 2019.
[27] C. Zhai, X. Chen, C. Yan, Y. Liu, and H. Li, "Ecological cooperative adaptive cruise control for a heterogeneous platoon of heavy-duty vehicles with time delays," *IEEE Access*, vol. 8, pp. 146208–146219, 2020.
[28] C. Dannheim, M. Mäder, C. Icking, J. Loewenau, and K. Massow, "TEAM—CO_2 reduction through online weather assistant for cooperative ACC driving," in *Proc. 5th Int. Conf. Comput. Intell., Commun. Syst., Netw. (CICSyN)*, Madrid, Spain, Jun. 2013, pp. 369–373. [Online]. Available: https://ieeexplore.ieee.org/document/6571394

HAO MA was born in 1997. He received the B.S. degree in vehicle engineering from Jilin University, Changchun, China, where he is currently pursuing continuous academic programme that involves postgraduate study in vehicle engineering. His research interests include pure electric vehicles, hybrid electric vehicles, and theory and optimal energy control strategy about new energy vehicles.

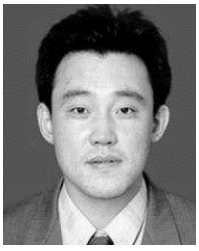

LIANG CHU (Member, IEEE) was born in 1967. He received the B.S., M.S., and Ph.D. degrees in vehicle engineering from Jilin University, Changchun, China. He is currently a Professor and the Doctoral Supervisor with the College of Automotive Engineering, Jilin University. His research interests include the driving and braking theory and control technology for hybrid electric vehicles, which conclude powertrain and brake energy recovery control theory and technology on electric vehicles and hybrid vehicles, theory and technology of hydraulic antilock braking and stability control for passenger cars, and the theory and technology of air brake ABS, and the stability control for commercial vehicle.

Dr. Chu has been a SAE Member. He was a member at the Teaching Committee of Mechatronics Discipline Committee of China Machinery Industry Education Association in 2006.

JIANHUA GUO was born in 1976. He received the Ph.D. degree in vehicle engineering, with a major in power machinery and engineering (internal combustion engine) from Jilin University, Changchun, China. He is currently a Professor with the College of Automotive Engineering, Jilin University. His main research interests include new energy vehicles, including hybrid electric vehicles, pure electric vehicles, control strategies, parameter matching, and powertrain control.

Since his graduation, he has participated in 14 projects at the National, Provincial, and Ministerial level and a total of over 40 articles published. Among them, ten papers were retrieved by SCI, 25 articles were retrieved by EI. Besides, he has 15 patents for invention. He edited or enrolled in a series of five books.

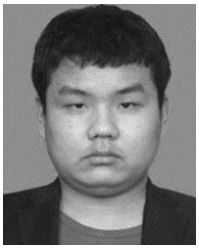

JIAWEI WANG was born in 1996. He received the B.S. degree in vehicle engineering from Jilin University, Changchun, China, where he is currently pursuing continuous academic programme that involves both postgraduate and doctoral study in vehicle engineering.

He has taken part in projects, which are Jilin Science and Technology Development Plan Project (20170204085GX), the 863 national high technology research and development program of China (2012AA110903), Jilin young talent plan project (20190103160JH) and Jilin industrial technology innovation strategic alliance project (20150309013GX). His research interests include control strategy of energy, intelligent systems engineering, and theory and optimal energy control strategy about electric vehicles.

CHONG GUO received the B.S., M.S., and Ph.D. degrees from Jilin University, Changchun, China.

He is currently a Postdoctoral Fellow with the College of Automotive Engineering, Jilin University. His current research interests include control strategies of key parts in electric vehicles, characteristic study on power batteries, and control strategies for electric vehicles.